Electronic Supplementary Information for:

Switching of the Triplet Excited State of Rhodamine-C_{60} Dyads

Fen Wang,[a,b,¶] Xiaoneng Cui,[a,¶] Zhangrong Lou,[a] Jianzhang Zhao,[a,] Ming Bao[a] and Xingwei Li[b*]*

[a] State Key Laboratory of Fine Chemicals Dalian University of Technology. Dalian 116024, P. R. China. Fax: (+) 86 411 8498 6236, E-mail: zhaojzh@dlut.edu.cn
Homepage: http://finechem.dlut.edu.cn/photochem

[b] Dalian Institute of Chemical Physics Chinese Academy of Sciences. Dalian 116023, P. R. China. E-mail: xwli@dicp.ac.cn

[¶] These authors contributed equally to this work.

Index

1.0 General information

All the chemicals used in synthesis are analytical pure and were used as received. Solvents were dried and distilled before used for synthesis. ^{1}H and ^{13}C chemical shifts are reported in parts per million (ppm) relative to TMS, with the residual solvent peak used as an internal reference. The mass spectra were measured by a MALDI and Agilent 6540 Q-Tof. UV-vis absorption spectra and kinetic curve (UV-vis absorption) were taken on a HP8453 UV-visible spectrophotometer. The fluorescence and kinetic curve (fluorescence emission) was recorded with a RF 5301PC spectrofluorometer. The spectra of measuring singlet oxygen quantum yields was measured in dichloromethane (DCM) with methylene blue (MB) (Φ = 0.57, in DCM) as the standard and 1,3-diphenylisobenzofuran (DPBF) as the $^{1}O_2$ scavenger.

The nanosecond time-resolved transient difference absorption spectra were measured on LP920 laser flash photolysis spectrometer (Edinburgh Instruments, UK) and recorded on a Tektronix TDS 3012B oscilloscope and with a nanosecond pulsed laser (OpoletteTM 355II+UV nanosecond pulsed laser, typical pulse length: 7 ns. Pulse repetition: 20 Hz. Peak OPO energy: 4 mJ. The wavelength is tunable in the range of 410–2200 nm. OPOTEK, USA). The lifetime values (by monitoring the decay trace of the transients) were obtained with the LP900 software. All samples in flash photolysis experiments were deaerated with N2 for ca. 15 min before measurement and the gas flow is kept during the measurement. For the samples with TFA added, the solution was standed for 1 h before measurement.

Cyclic voltammetry was performed using a CHI610D Electrochemical workstation (Shanghai, China). Cyclic voltammograms were recorded at scan rates of 0.1 V/s. The electrolytic cell used was a three electrodes cell. Electrochemical measurements were performed at RT using 0.1 M tetrabutylammonium hexafluorophosphate ($Bu_4N[PF_6]$) as supporting electrolyte. The solution was purged with N_2 before measurement. The working electrode was a glassy carbon electrode, and the counter electrode was platinum electrode. A nonaqueous Ag/ $AgNO_3$ (0.1 M in acetonitrile) reference electrode was contained in a separate compartment connected to the solution via semipermeable membrane. DCM and Toluene were used as the solvent. Ferrocene was added as the internal references.

Intracellular singlet oxygen ($^1O_2$) detection upon visible irradiation: HeLa (human cervical cancer) cell lines were obtained from ATCC cultured in Dulbecco's modified Eagle's medium (Invitrogen, Auckland, New Zealand) containing 10% fetal bovine serum (Hyclone, Beijing, China) and penicillin-streptomycin (100 U/ml penicillin and 0.1 mg/ml streptomycin). Cells were incubated at 37°C in a humidified incubator (SANYO, MCO-15AC, Japan) with 5% CO_2. After the Hela cells were incubated with **RB-C_{60}-1** (**RB-C_{60}-2**) and washed three times with phosphate buffered saline (PBS, Gibco, pH = 7.4), they were further incubated with 10 μM DCFH-DA for 2 min and irradiated with a 515–525 nm LED for 3 min at 37 °C to perform the fluorescence detection of DCF with FV1000 Confocal microscopy (Olympus) with an objective lens (×20), respectively. Other information is available in the Figure captions.

Intracellular photodynamic studies: Hela cells and COS-7 cells' culture were same to cellular ROS Detection during Irradiation experiments. Prior to imaging, the medium was removed. Cell imaging was carried out after washing cells with phosphate buffered saline (PBS, Gibco, pH = 7.4) for three times and 1 mL PBS was added to Laser scanning confocal Petri dish (nest, Glass bottom diameter: 20 mm). Then the cells were irradiated with a 515–525 nm LED for 30 min (**RB-C_{60}-1, RB-C60-2**) at 37 °C. Afterwards, the cells were stained with Trypan blue (100 μL 0.4% Trypan blue was added), three minutes later, the cell images were acquired on IX81 confocal laser-scanning microscope (Olympus) with an objective lens (×20 and ×10). Other information is available in the Figure captions.

2.0 Synthesis

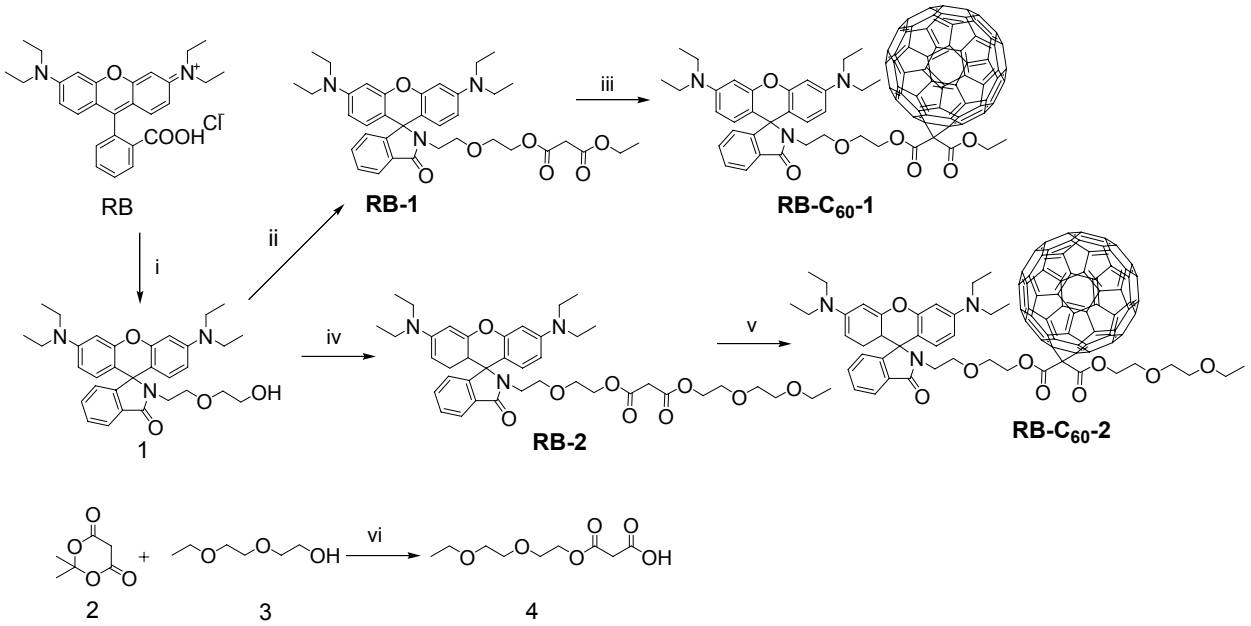

Scheme S1. Synthesis of the Triplet Photosensitizers **RB-C60-1** and **RB-C60-2**. (i) (a). $POCl_3$, dry DCE, reflux, 8 h; (b). 2-(2-aminoethoxy)ethanol, triethylamine, dry THF, rt, 8 h.; yield: 60%. (ii) ethyl malonyl chloride, pyridine, dry DCM, rt, overnight; yield: 75 %. (iii) C_{60}, I_2, DBU, toluene, rt, overnight; yield: 57%. (iv) 4, DMAP, DCC, dry DCM, rt, 24 h; yield: 76 %. (v) C_{60}, I_2, DBU, toluene, rt, overnight; yield: 55%. (vi) 120 °C, 3 h.

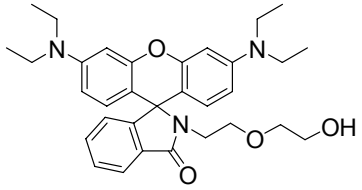

1

Compound 1: To a solution of rhodamine **B** acid (239.1 mg, 0.5 mmol) in dry 1, 2-dichloroethane (10.0 mL) at room temperature, phosphorus oxychloride (0.25 mL) was added dropwise over a period of 5 min. After being refluxed for 8 h, the reaction mixture was cooled and concentrated under reduced pressure to give rhodamine B acid chloride. Without further purification, the resulting acid chloride was dissolved in dry THF (10 mL), and then was added dropwise to a solution of 2-(2-aminoethoxy)ethanol (0.6 mmol) in dry THF (10 ml) containing triethylamine (1 mL). After stirring for 8 h at room temperature, the mixture was concentrated under reduced pressure and the crude product was purified by column chromatography (silica gel, CH_2Cl_2) to give compounds **1** as a pink-white solid. Yield: 193.2 mg, 73%. ^{1}H NMR (400 MHz, $CDCl_3$) δ 7.91–7.89 (m, 1H), 7.44–7.42 (m, 2H), 7.08–7.06 (m, 1H), 6.45 (d, J = 8.8 Hz, 2H), 6.38 (d, J = 2.1 Hz, 2H), 6.28 (dd, J = 8.9, 2.4 Hz, 2H), 3.56 (s, 2H), 3.36–3.31(m, 12H), 3.20 (t, J = 6.3 Hz, 2H), 2.51(br, 1H), 1.17 (t, J = 7.0 Hz, 12H). ^{13}C NMR (100 MHz, $CDCl_3$) δ 168.5, 153.6, 153.3, 148.8, 132.4, 131.1, 128.9, 128.0, 123.8, 122.9, 108.1, 105.7, 97.8, 72.0, 68.4, 65.0, 61.7, 44.4, 39.8, 12.6. HRMS: m/z: [M + H]$^+$ calculated for $C_{32}H_{40}N_3O_4$: 530.3019, found 530.3015.

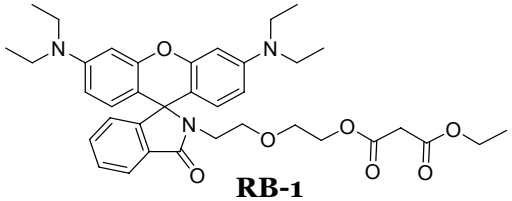

RB-1

Synthesis of compound RB-1: Compound **1** (105.8mg, 0.2 mmol) was dissolved in dry CH_2Cl_2 (40 ml) and pyridine (96 µL, 1.2 mmol) was added under Ar atmosphere. The mixture was cooled on an ice bath and methyl malonyl chloride (28 µL, 0.24mmol) in CH_2Cl_2 (20 ml) was added dropwise. The mixture was

stirred for 12 h at room temperature. The crude product was purified by column chromatography (silica gel, MeOH:CH_2Cl_2=1:30, v/v). Yield: 96.5 mg, 75%. ^{1}H NMR (400 MHz, $CDCl_3$) δ 7.96–7.93 (m, 1H), 7.53–7.44 (m, 2H), 7.17–7.10 (m, 1H), 6.50 (s, 1H), 6.48 (s, 1H), 6.43 (d, *J* = 2.2 Hz, 2H), 6.33 (dd, *J* = 8.9, 2.3 Hz, 2H), 4.22 (dd, *J* = 14.3, 7.2 Hz, 2H), 4.18 (t, *J* = 4.6 Hz, 2H), 3.48 (t, *J* = 4.7 Hz, 2H), 3.42–3.37 (m, 12H), 3.25 (t, *J* = 7.1 Hz, 2H), 1.30 (t, *J* = 7.1 Hz, 3H), 1.22 (t, *J* = 7.0 Hz, 12H). ^{13}C NMR (100 MHz, $CDCl_3$) δ 168.2, 166.6, 166.4, 153.7, 153.2, 148.7, 132.4, 130.9 , 128.8, 127.9, 123.7, 122.7, 108.0, 105.5, 97.7, 68.0, 67.9, 64.8, 64.5, 61.4, 44.3, 41.4, 39.2, 14.0, 12.6. HRMS: *m*/*z*: $[M + H]^+$ calculated for $C_{37}H_{46}N_3O_7$: 644.3336, found 644.3366.

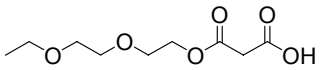

4

Synthesis of compound 4: A mixture of meldrum's acid (721 mg, 5.0 mmol) and 2-(2-Ethoxyethoxy)ethanol (670.9 mg, 5.0 mmol) was heated under stirring in an open flask to 120 °C for 3 h. **4** can be used without further purification. Yield: 900 mg , 82%.

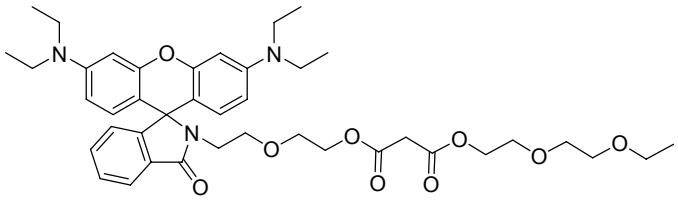

RB-2

Synthesis of compound RB-2: Under N_2 atmosphere, the mixture of compound **1** (105.8 mg, 0.2 mmol) and compound **4** (44.0 mg, 0.2 mmol) in dry CH_2Cl_2 (15 mL) was cooled to 0 °C. 4-dimethylaminopyridine (DMAP, 2.4 mg, 0.02 mmol) and Dicyclohexylcarbodiimide (DCC, 41.3 mg, 0.2 mmol) were added subsequently. Then the solution was stirred for 1 h at 0 °C, it was left at room temperature for another 24 h. Progress of the reaction was monitored by TLC. After evaporation of the

solvent, the resulting product was purified by column chromatography (silica gel, MeOH:CH_2Cl_2=1:50, v/v). 111.2 mg of **RB-2** was obtained. Yield: 76%. ^{1}H NMR (400 MHz, $CDCl_3$) δ 7.90–7.87 (m, 1H), 7.44–7.40 (m, 2H), 7.08–7.04 (m, 1H), 6.44 (s, 1H), 6.42 (s, 1H), 6.38 (d, *J* = 2.2 Hz, 2H), 6.27 (dd, *J* = 8.9, 2.3 Hz, 2H), 4.27 (t, *J* = 4.8 Hz, 2H), 4.11 (t, *J* = 4.7 Hz, 2H), 3.69 (t, *J* = 4.9 Hz, 2H), 3.63–3.61 (m, 2H), 3.58–3.56 (m, 2H), 3.51 (dd, *J* = 14, 7.0 Hz, 2H), 3.41 (t, *J* = 4.8 Hz, 2H), 3.38 (s, 2H), 3.34 (dd, *J* = 13.7, 6.7 Hz, 10H), 3.20 (t, *J* = 7.0 Hz, 2H) 1.22–1.15 (m, 15H). ^{13}C NMR (125 MHz, $CDCl_3$) δ 168.2, 166.4, 166.38, 153.7, 153.3, 148.8, 132.3, 131.0, 128.8, 127.9, 123.8, 122.7, 108.1, 105.6, 97.8, 70.7, 69.8, 68.8, 68.1, 68.8, 66.6, 64.8, 64.54, 64.51, 44.3, 41.2, 39.2, 15.1, 12.6. HRMS: *m*/*z*: $[M + H]^+$ calculated for $C_{41}H_{54}N_3O_9$: 732.3860, found: 732.3884.

General approach for the synthesis of compounds RB-C_{60}-1 and RB-C_{60}-2:

Iodine (18 mg, 0.07mmol) was added to a solution of C_{60} (50.9mg, 0.07 mmol) in toluene (50 mL). The solution of **RB-1** in toluene (40 mL) was added. 1,8-Diazabicyclo[5.4.0]undec-7-ene (21.3 mg, 0.14 mmol) in toluene (30 ml) was added dropwise within 1 h and the reaction mixture was stirred overnight at room temperature. The reside crude was purified by column chromatography (silica gel, MeOH:CH_2Cl_2=1:100, v/v) to afford the desired compound as a dark solid. **RB-C_{60}-2** was prepared with similar method.

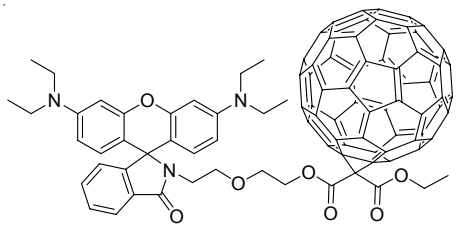

RB-C_{60}-1

Yield: 54.4 mg (57%). dark power. M.p. 162-165 °C. ^{1}H NMR (400 MHz, $CDCl_3$) δ 7.90–7.86 (m, 1H), 7.44–7.39 (m, 2H), 7.07–7.03 (m, 1H), 6.44 (s, 1H), 6.42 (s, 1H), 6.37 (d, *J* = 2.1 Hz, 2H), 6.26 (dd, *J* = 8.9, 2.3 Hz, 2H), 4.50 (dd, *J* = 14.4, 7.3 Hz, 2H), 4.46 (t, *J* = 4.6 Hz, 2H), 3.59 (t, *J* = 4.5 Hz, 2H), 3.33 (dd, *J* = 13.8, 6.7 Hz, 10H), 3.26 (t, *J* = 6.3 Hz, 2H), 1.43 (t, *J* = 7.1 Hz, 3H), 1.16 (t, *J* = 7.0 Hz, 12H). ^{13}C NMR (100 MHz, $CDCl_3$) δ 168.3, 163.6, 168.3, 153.8, 153.2, 148.7, 145.3, 145.21, 145.19, 145.14, 145.09, 144.8, 144.63, 144.60, 144.56, 144.53, 144.50, 143.8, 142.98, 142.96, 142.93, 142.91, 142.87, 142.2, 142.1, 141.81, 141.80,

140.8, 139.2, 138.9, 132.4, 130.7, 128.7, 127.9, 123.7, 122.7, 108.0, 105.5, 97.8, 71.5, 68.0, 67.9, 66.1, 64.8, 63.4, 44.3, 39.3, 14.2, 12.6. HRMS (MALDI-TOF): *m/z*: [M+ H]$^+$ calculated for $C_{97}H_{44}N_3O_7$: 1362.3179, found 1362.3141.

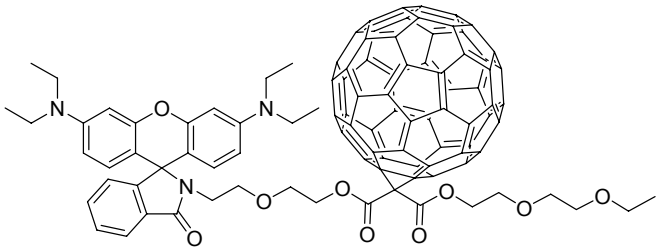

RB-C_{60}-2

Yield: 55.9 mg (55%). Dark power. M.p. 103-106 °C. ^{1}H NMR (400 MHz, $CDCl_3$) δ 7.89–7.85 (m, 1H), 7.43–7.39 (m, 2H), 7.06–7.02 (m, 1H), 6.43 (s, 1H), 6.41 (s, 1H), 6.36 (d, *J* = 2.1 Hz, 2H), 6.26 (dd, *J* = 8.8, 2.1 Hz, 2H), 4.61(t, *J* = 4.4 Hz, 2H), 4.46 (t, *J* = 4.5 Hz, 2H), 3.84 (t, *J* = 6.0 Hz, 2H), 3.66 (t, *J* = 4.8 Hz, 2H), 3.60–3.54 (m, 4H), 3.50 (dd, *J* = 14.0, 7.0 Hz, 2H), 3.32 (dd, *J* = 14.0, 7.0 Hz, 10H), 3.25 (t, *J* = 6.0 Hz, 2H), 1.17 (m, 15H). ^{13}C NMR (100 MHz, $CDCl_3$): δ 168.3, 163.5, 163.4, 153.8, 153.2, 148.7, 145.26, 145.25, 145.2, 145.14, 145.10, 145.08, 144.8, 144.6, 144.55, 144.53, 144.50, 143.8, 142.98, 142.94(two overlapping), 142.91, 142.86, 142.2, 142.1, 141.8, 141.78, 140.82, 140.78, 139.1, 139.0, 132.4, 130.7, 128.7, 127.9, 123.7, 122.7, 108.0, 105.5, 97.9, 71.4, 70.7, 69.8, 68.7, 68.0, 67.8, 66.7, 66.2, 66.1, 64.9, 44.3, 39.3, 15.2, 12.7. HRMS(MALDI-TOF): *m/z*: $[C_{101}H_{51}N_3O_9]^-$ calculated for: 1449.3710, found 1449.3625.

3.0 NMR and HR-MS spectra

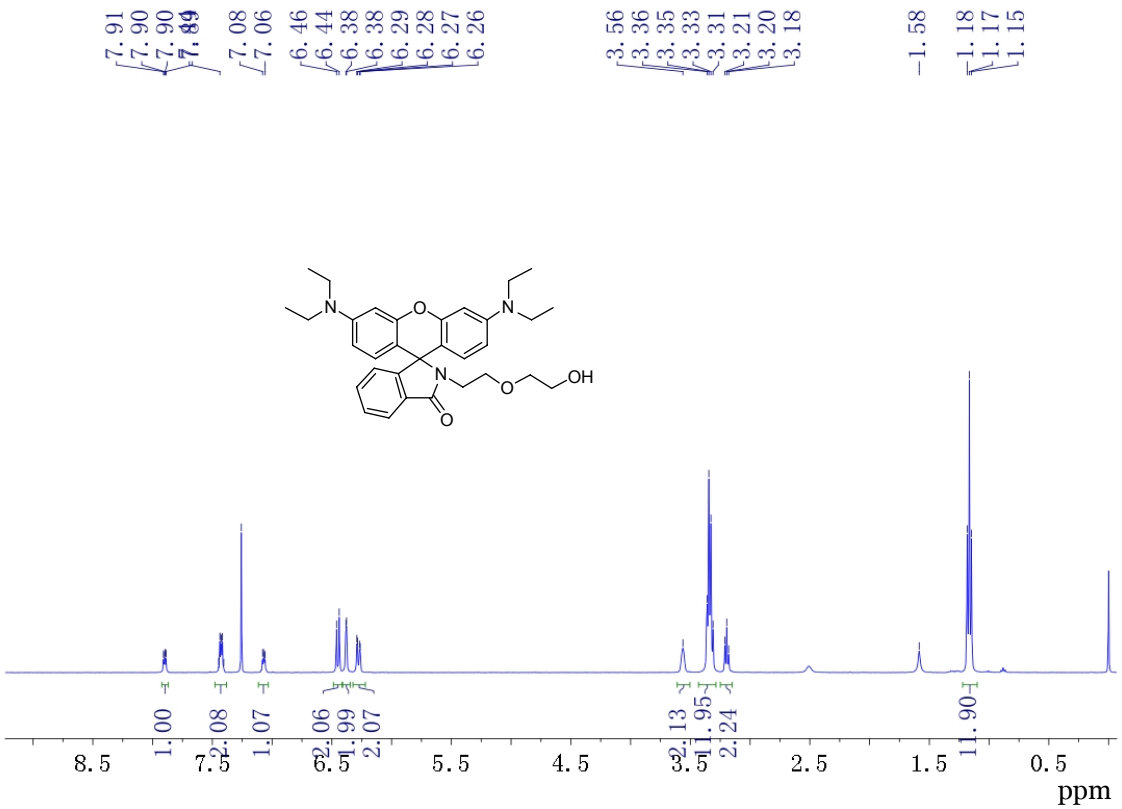

Figure S1. ^{1}H NMR of **1** (400 MHz, $CDCl_3$).

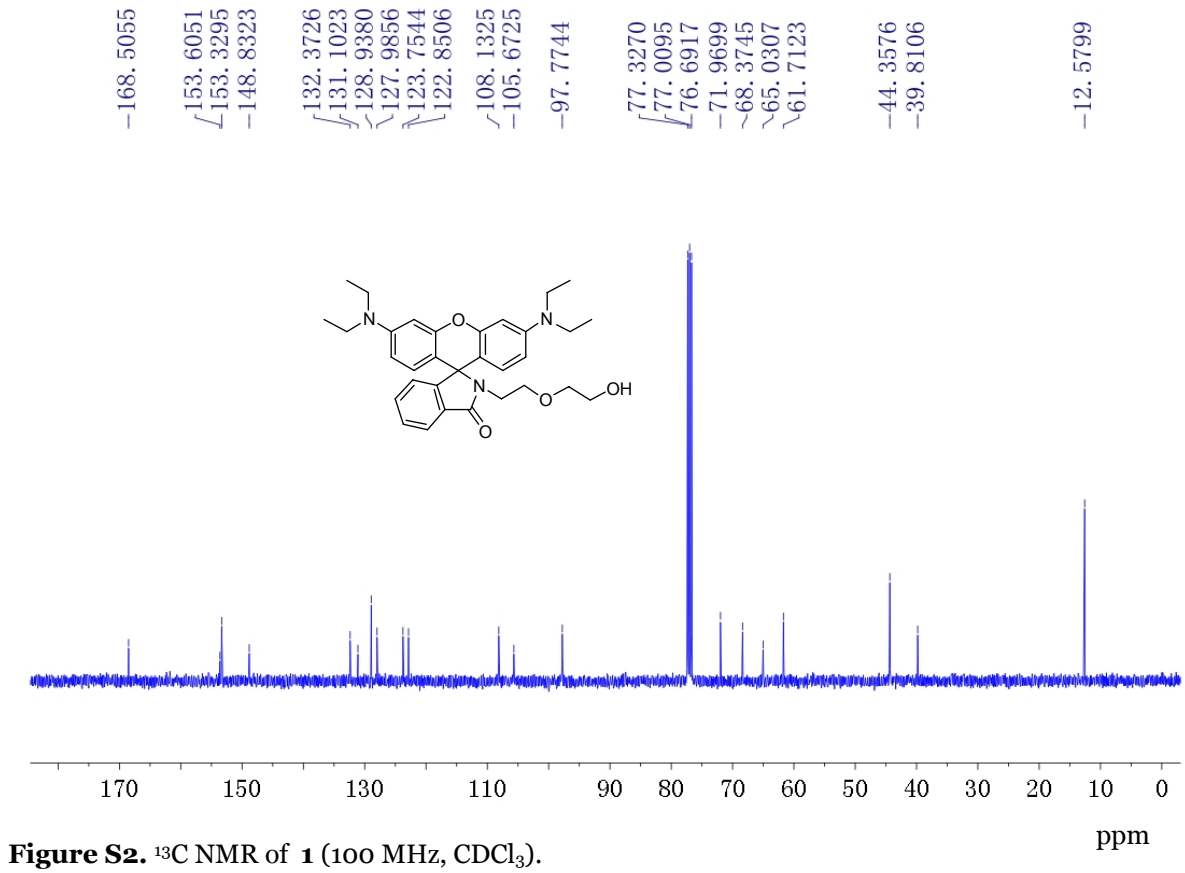

Figure S2. ^{13}C NMR of **1** (100 MHz, $CDCl_3$).

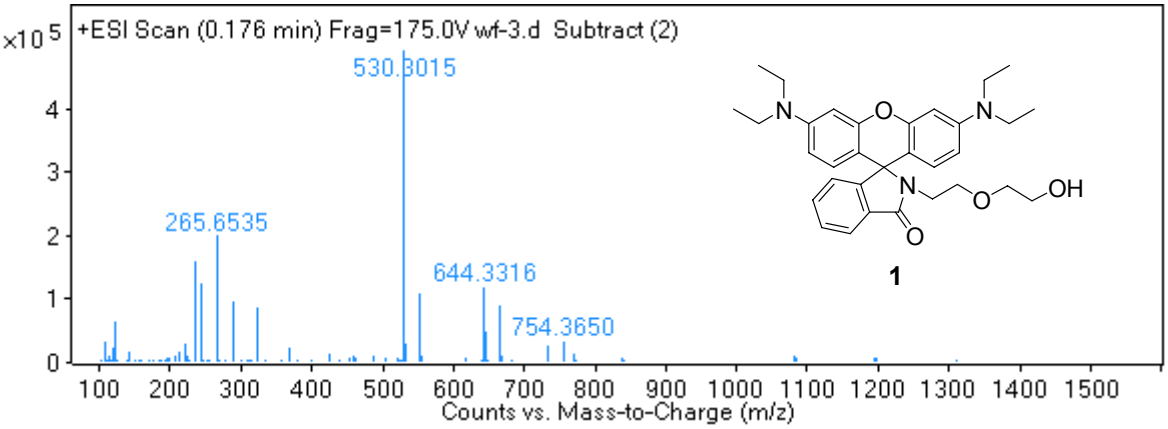

Figure S3. HRMS ESI of **1**.

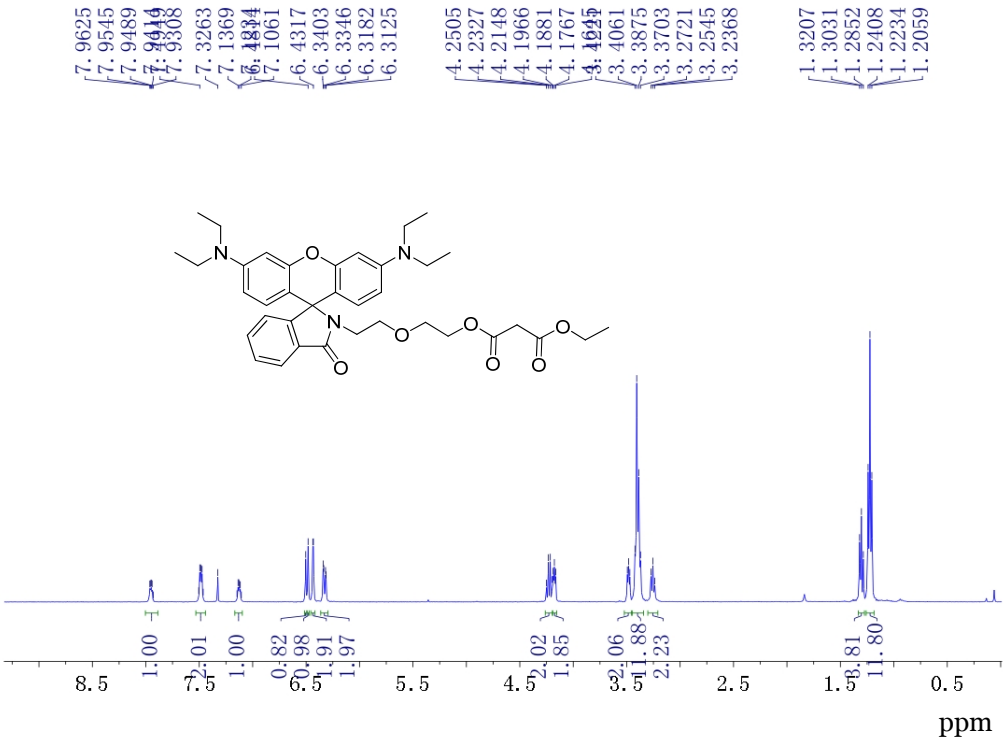

Figure S4. ^{1}H NMR of **RB-1** (400 MHz, $CDCl_3$).

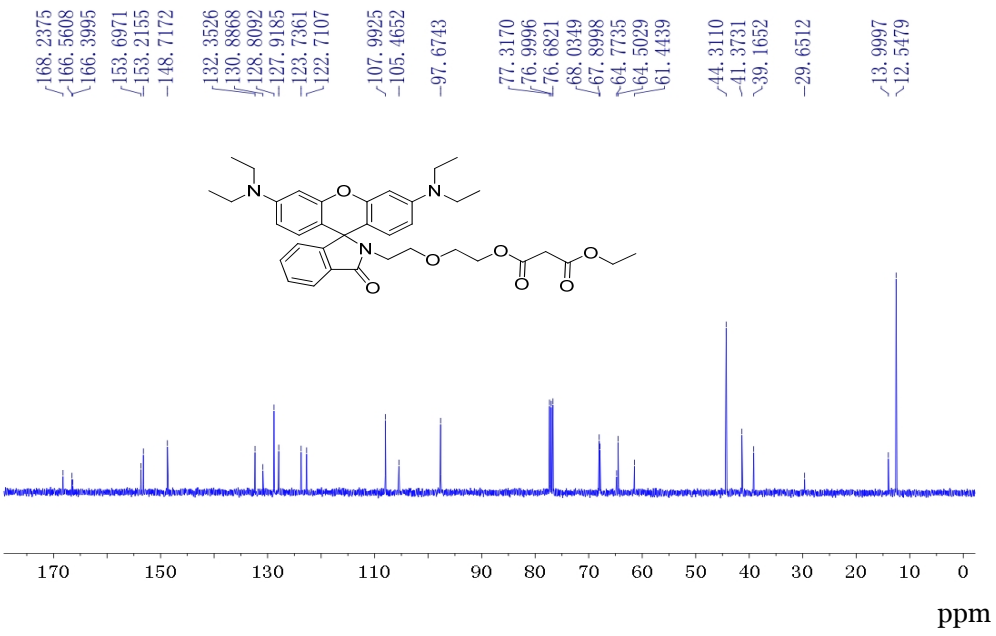

Figure S5. ^{13}C NMR of **RB-1** (100 MHz, $CDCl_3$).

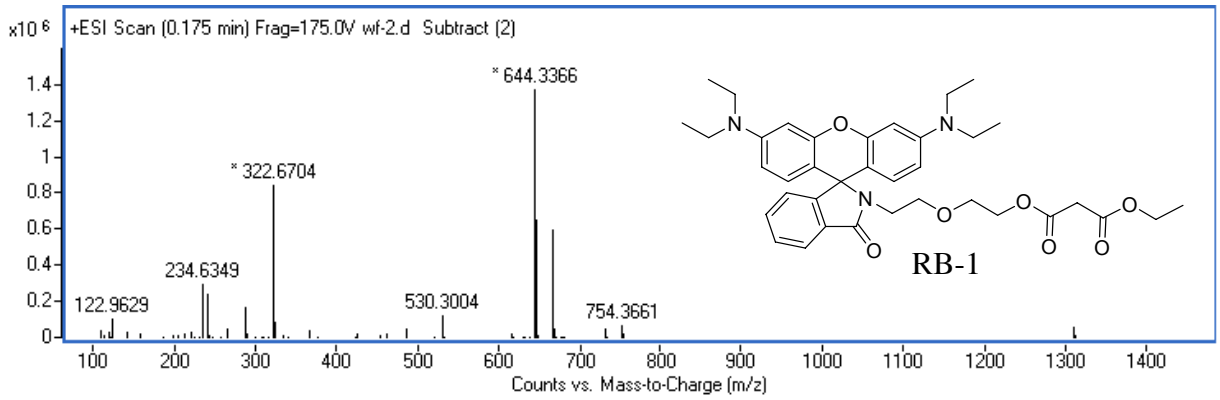

Figure S6. HRMS ESI of **RB-1**.

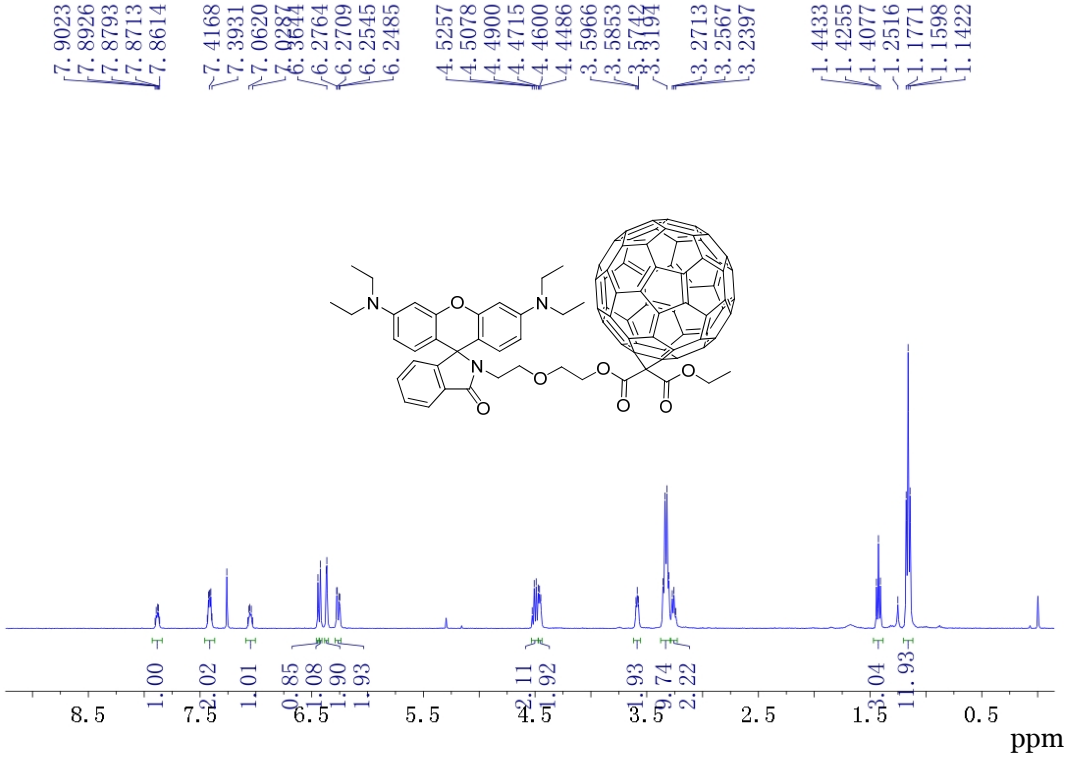

Figure S7. ^{1}H NMR of **RB-C_{60}-1** (400 MHz, $CDCl_3$).

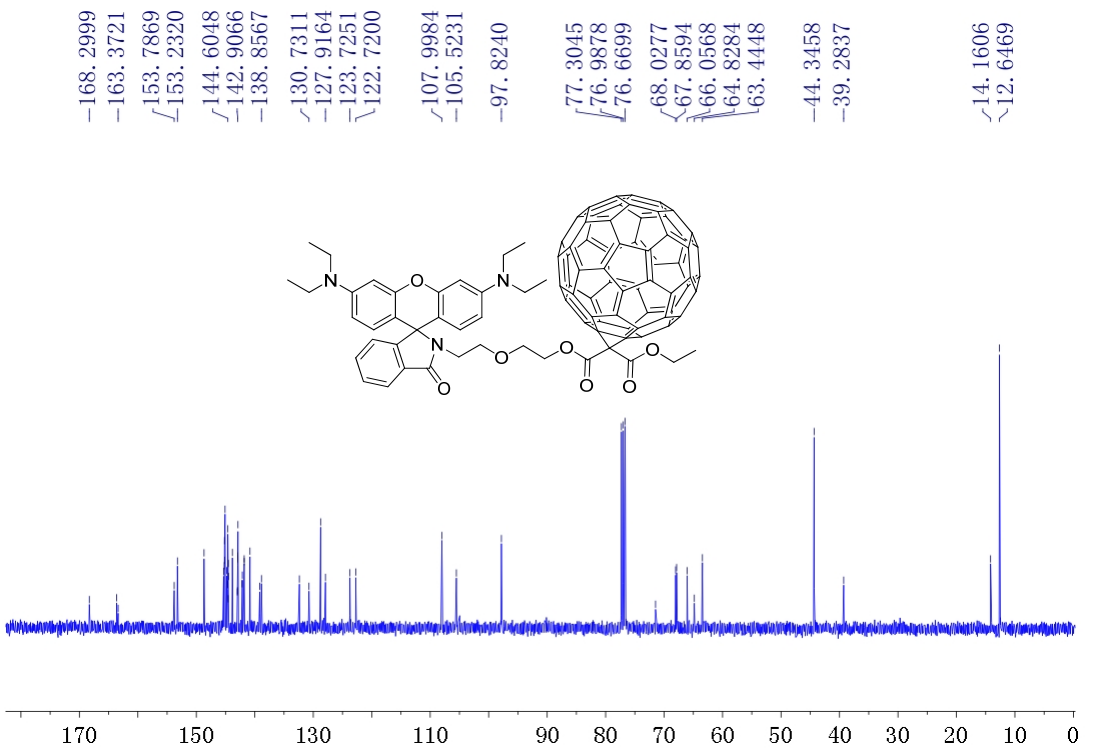

Figure S8. ^{13}C NMR of **RB-C60-1** (400 MHz, $CDCl_3$).

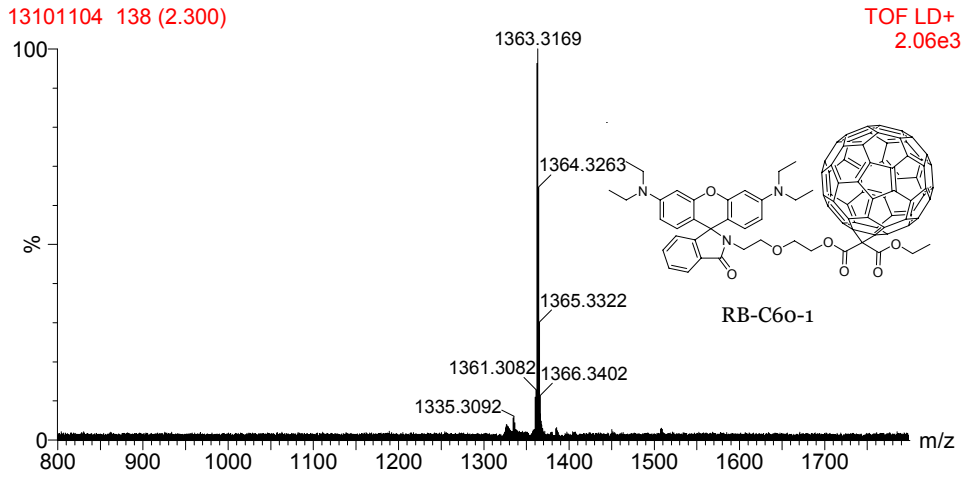

Figure S9. MALDI-HRMS ESI of **RB-C_{60}-1**.

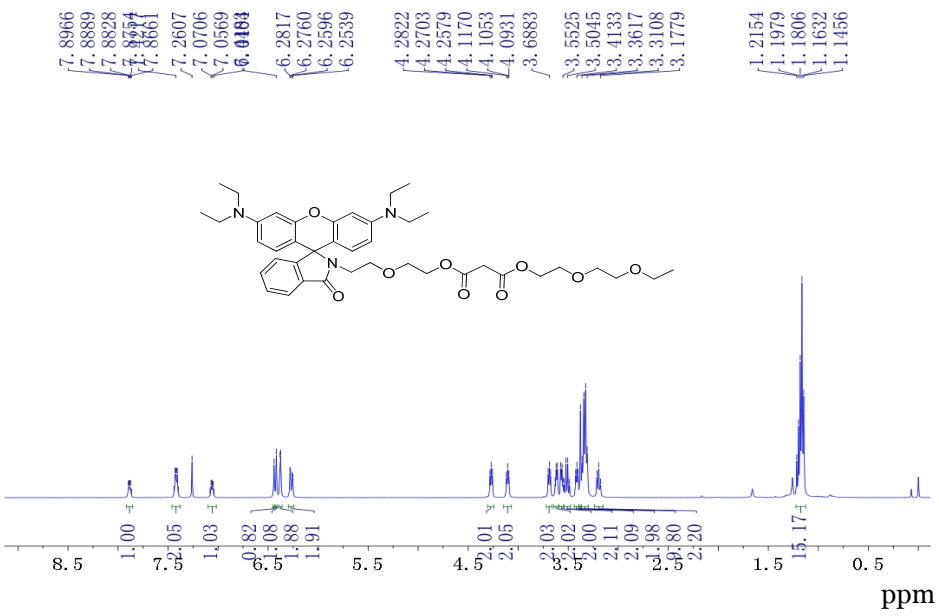

Figure S10. ^{1}H NMR of **RB- 2** (400 MHz, $CDCl_3$).

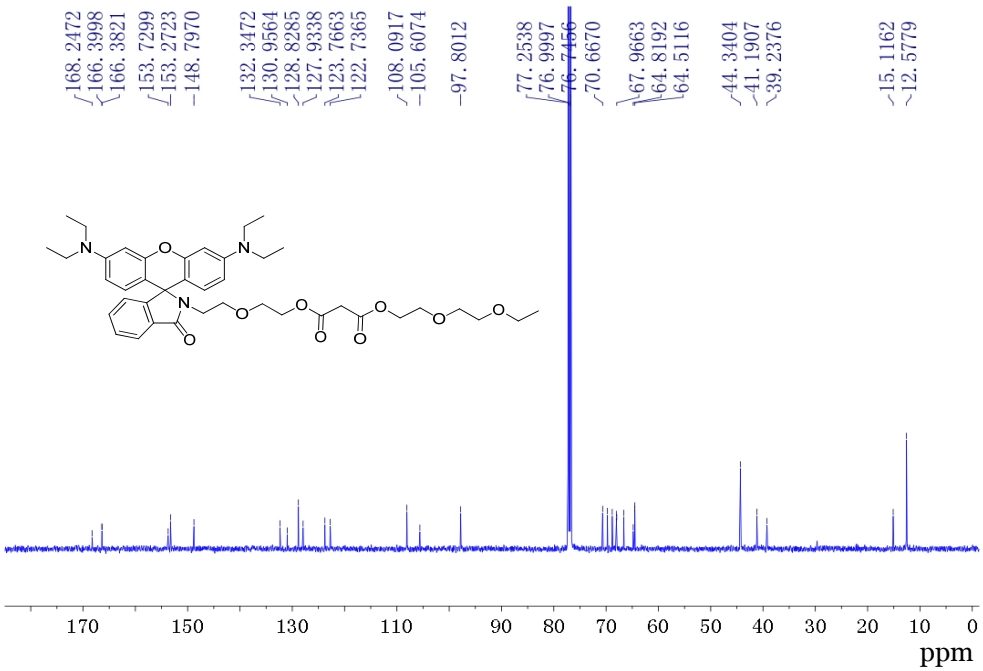

Figure S11. ^{13}C NMR of **RB- 2** (125 MHz, $CDCl_3$).

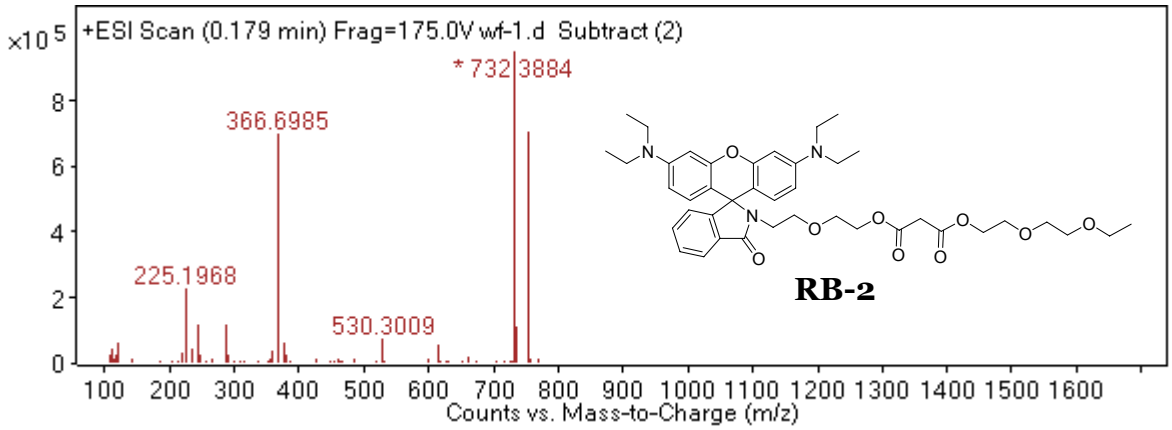

Figure S12. HRMS ESI of **RB-2**.

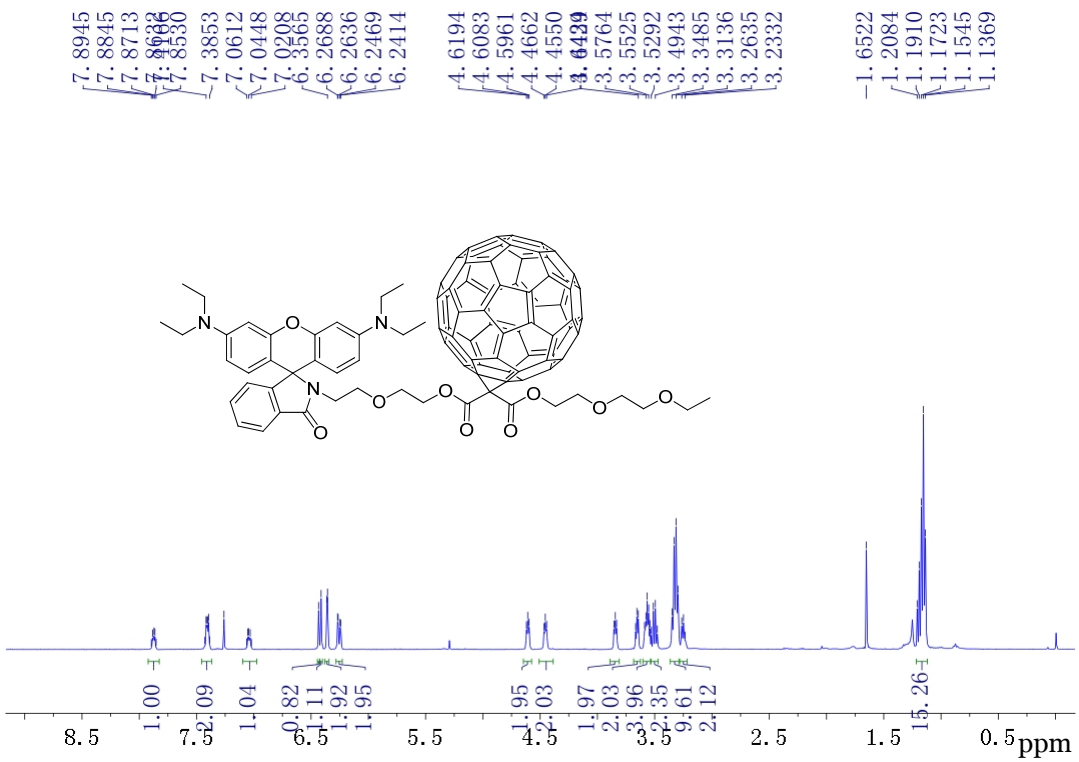

Figure S13. ^{1}H NMR of **RB-C$_{60}$-2** (400 MHz, $CDCl_3$).

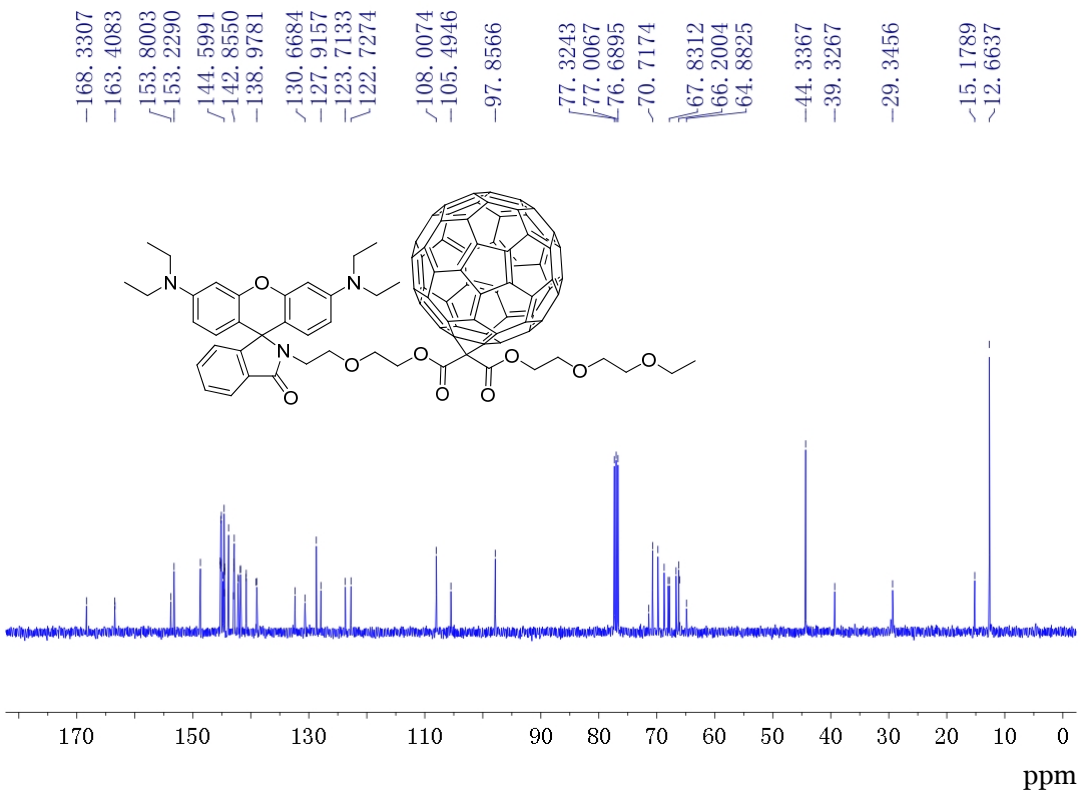

Figure S14. ^{13}C NMR of **RB-C_{60}-2** (400 MHz, $CDCl_3$).

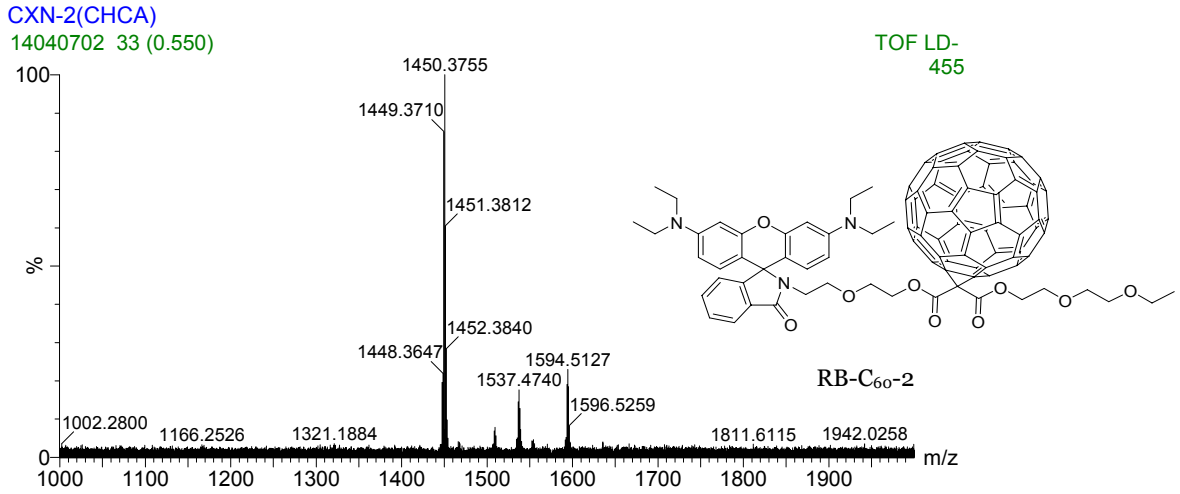

Figure S15. MALDI-HRMS ESI of **RB-C_{60}-2**.

4.0 The UV-Vis absorption and emission spectra

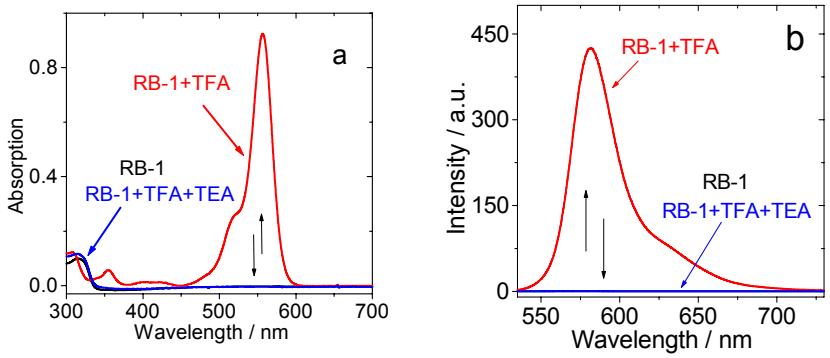

Figure S16. UV-Vis absorption spectra and emission spectra of the compounds **RB-1**. In DCM:CH3OH (9:1, v/v). With addition of TFA (5.0 mol/L, 50 μL), or TEA (neat, 50 μL) for the switching purpose. c = 1.0 ×10^{-5} M. 20 °C.

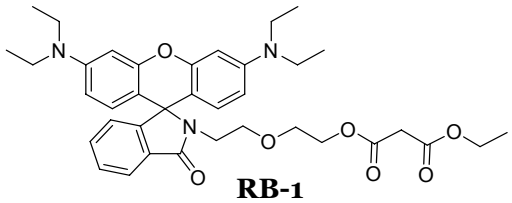

RB-1

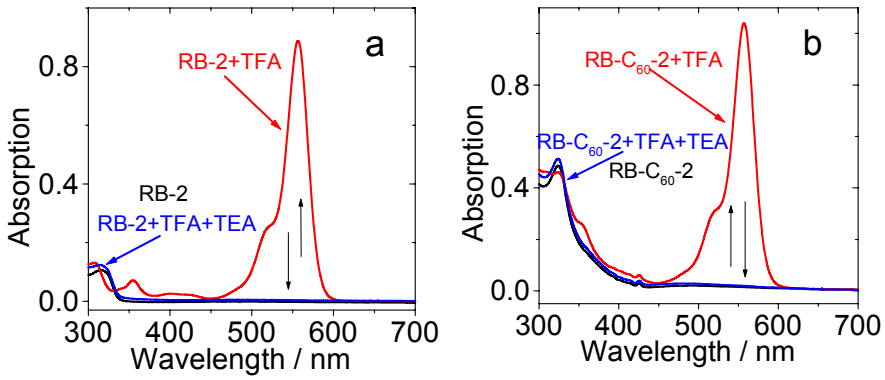

Figure S17. UV-Vis absorption spectra of the compounds **(a) RB-2, (b) RB-C60-2**. In DCM:CH3OH (9:1, v/v). With addition of TFA (5.0 mol/L, 50 μL), or TEA (neat, 50 μL) for the switching purpose. c = 1.0 ×10^{-5} M. 20 °C.

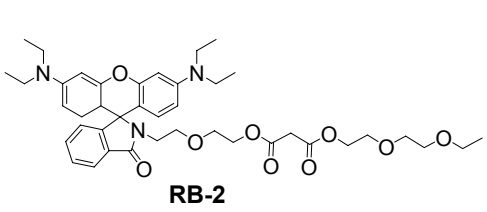

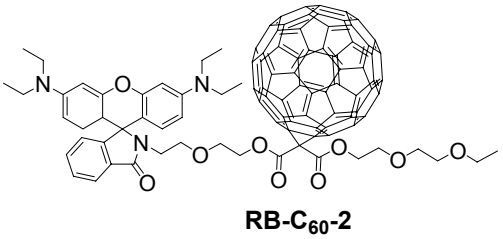

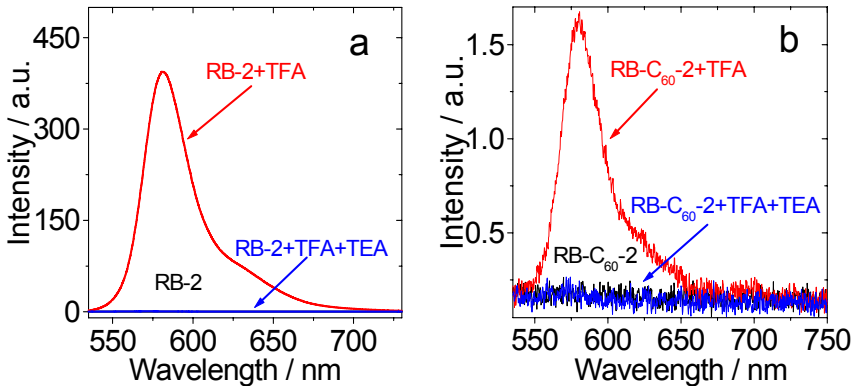

Figure S18. The fluorescence emission spectra of (a) **RB-2.** (b) **RB-C₆₀-2**. λex = 535 nm (In MeOH : DCM = 1 : 9, v/v). With addition of TFA (5.0 mol/L, 50 μL), or TEA (neat, 50 μL) added for the switching purpose. c = 1.0 × 10⁻⁵ M; 20 °C.

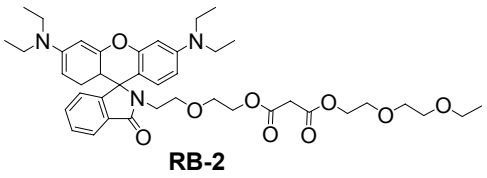

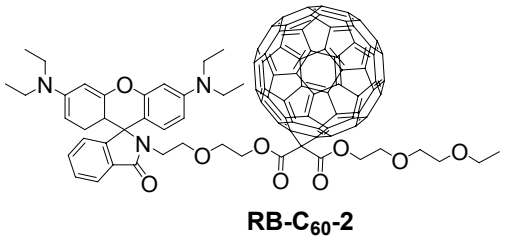

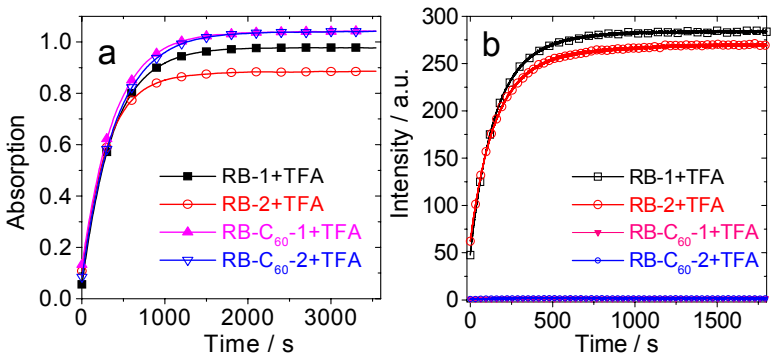

Figure S19. (a) Kinetics of the spiro lactam →opened amide transformation of the Rhodamine moiety in different compounds, monitored by following the absorption at 557 nm upon addition of TFA (5.0 mol/L, 50 μL) into the solution of compounds **RB-1**, **RB-2**, **RB-C60-1**, **RB-C60-2**. In DCM:CH3OH (9:1, v/v). c = 1.0 × 10^{-5} M. 20 °C. (b) Kinetic curve (fluorescence emission) of compound **RB-1**, **RB-2, RB-C60-1**, **RB-C60-2.** In DCM:CH3OH = 9:1 (v/v) with TFA (5.0 mol/L, 50 μL) added. Trace of the emission intensity at 580 nm. λ_{ex} = 535 nm. c = 1.0 ×10^{-5} M. 20 °C.

5.0 Cyclic voltammogram

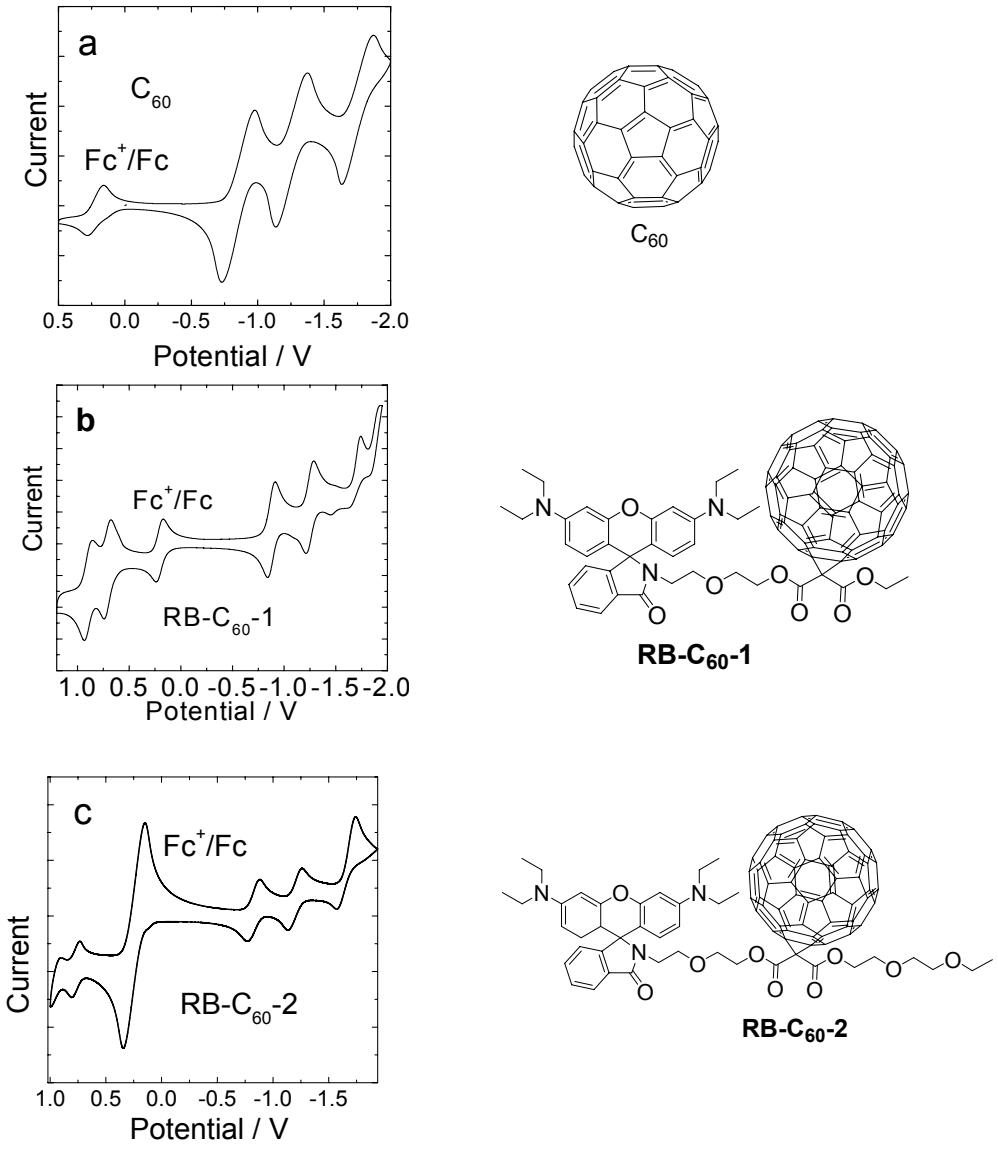

Figure S20. Cyclic voltammogram of the dyad photosensitizer **C_{60}, RB-C_{60}-1, RB-C_{60}-2** as the reference compounds for the singlet energy donor and acceptor, respectively. (a) compound C_{60}, in toluene/DCM(1/1) solutions containing 1.0 mM photosensitizers with the ferrocene, 0.10 M Bu_4NPF_6 as supporting electrolyte. (b) compound **RB-C_{60}-1**, in DCM solutions containing 0.5 mM photosensitizers with the ferrocene, 0.10 M Bu_4NPF_6 as supporting electrolyte. (c) compound **RB-C_{60}-2** in DCM solutions containing 0.5 mM photosensitizers with the ferrocene, 0.10 M Bu_4NPF_6 as supporting electrolyte, Scan rate: 0.1 V/s.

6.0 Calculation of the free energy changes of the electron transfer

The free energy changes of the electron transfer process (charge separation, CS), can be calculated with the Weller equation (Eq. 1 and Eq. 2).

$$\Delta G^{0}{}_{\mathrm{CS}} = e[E_{OX} - E_{RED}] - E_{00} + \Delta G_{\mathrm{S}} \qquad \text{(Eq. 1)}$$

$$\Delta G_{\mathrm{S}} = -\frac{e^2}{4\pi\varepsilon_{\mathrm{S}}\varepsilon_0 R_{\mathrm{CC}}} - \frac{e^2}{8\pi\varepsilon_0}\left(\frac{1}{R_D} + \frac{1}{R_{\mathrm{A}}}\right)\left(\frac{1}{\varepsilon_{REF}} - \frac{1}{\varepsilon_S}\right) \qquad \text{(Eq. 2)}$$

e = electronic charge, E_{OX} = half-wave potential for one-electron oxidation of the electron-donor unit, E_{RED} = half-wave potential for one-electron reduction of the electron-acceptor unit; note herein the anodic and peak potentials were used because in some cases the oxidation is irreversible therefore the formal potential $E_{1/2}$ cannot be derived; E_{oo} = energy level approximated with the fluorescence emission wavelength (for the singlet excited state) or the T1 state energy of C60. ε_S = static dielectric constant of the solvent, R_{CC} = center-to-center separation distance determined by DFT optimization of the geometry (The value of R_{CC} is 15.2 Å.), R_D is the radius of the donor, R_A is the radius of the electron acceptor, ε_{REF} is the static dielectric constant of the solvent used for the electrochemical studies, ε_o permittivity of free space (ε_o = 8.854 × 10^{-12} F/m). The solvents used in the calculation of free energy of the electron transfer is DCM (ε = 8.9, 20°C).

The value of ΔG_S for **RB-C_{60}-1** and **RB-C_{60}-2** is – 0.106 eV

For **RB-C_{60}-1**, with **C_{60}** as electron Acceptor,

ΔG(cs) = 0.71- (-0.88) – 1.72 + (-0.106)= – 0.24 eV (energy level approximated with the fluorescence emission wavelength of C60 (the singlet excited state)).

ΔG(cs) = 0.71- (-0.88) – 1.50 + (-0.106)= – 0.016 eV (energy level approximated with the triplet excited state of C60).

In the presence of TFA, For **RB-C_{60}-1**, with **C_{60}** as electron Acceptor,

ΔG(cs) = 0.85 – (-0.88) – 2.12 + (-0.106)= – 0.50 eV (energy level approximated with the fluorescence emission wavelength of RB-0 (the singlet excited state)).

ΔG(cs) = 0.85- (-0.88) – 1.50 + (-0.106)= + 0.12 eV (energy level approximated with the triplet excited state of C60).

For **RB-C60-2**, with **C60** as electron Acceptor,

ΔG(cs) = 0.77- (-0.83) – 1.72 + (-0.106)= – 0.23 eV (energy level approximated with the fluorescence emission wavelength of C60 (the singlet excited state)).

ΔG(cs) = 0.77- (-0.83) – 1.50 + (-0.106)= – 0.006 eV (energy level approximated with the triplet excited state of C60)

In the presence of TFA, For **R-BC$_{60}$-2**, with **C$_{60}$** as electron Acceptor,

ΔG(cs) = 0.85- (-0.83) – 2.12 + (–0.106)= – 0.55 eV (energy level approximated with the fluorescence emission wavelength of RB-0 (the singlet excited state)).

ΔG(cs) = 0.85- (-0.83) – 1.50 + (–0.106)= + 0.074 eV (energy level approximated with the triplet excited state of C60).

Table S1. Redox potentials of acceptors for study of the potential intramolecular electron transfer by the estimation of free-energy changes for the charge separation ΔG_{ET} (PET). Anodic and cathodic peak potential were presented. The potential values of the compounds with Fc as internal reference.[a]

	$E_{(OX)}$ (V)	$E_{(RED)}$ (V)	ΔGcs (eV)
Rhodamine B [c]	+0.85/+0.97	–1.15/–1.37	- [b]
C$_{60}$	- [b]	–0.86 / –1.26 / –1.75	- [b]
RB-C$_{60}$-1	+0.89 / +0.71	–0.88 / –1.25 / –1.69	–0.24[d]/–0.016[e]/–0.50[f] /+0.12[g]
RB-C$_{60}$-2	+0.95 / +0.77	–0.83 / –1.20 / –1.66	–0.13[d]/–0.006[e]/–0.55[f] /+0.074[g]

[a] Cyclic voltammetry in Ar saturated CH_2Cl_2 containing a 0.10 M $Bu_4N[PF_6]$ supporting electrolyte; Counter electrode is Pt electrode; working electrode is glassy carbon electrode; $Ag/AgNO_3$ couple as the reference electrode. [b] standing for no reduction potential and no ΔGcs value. [c] $[Ag^+]$ = 0.1 M. in DCM, 20 °C. Conditions: 1.0 mM dyad photosensitizers and 1.0 mM ferrocene in DCM, 293 K. [d] The value was calculated with the singlet excited state of C_{60} as $E_{0,0}$. [e] The value was calculated by triplet excited state of C_{60}. [f] With the S_1 state energy level of RB-0 as $E_{0,0}$ (2.12 eV); [g] With RB-0 as electron donor, and the T_1 state energy level of C_{60} as $E_{0,0}$.

7.0 Nanosecond time-resolved transient difference absorption spectra.

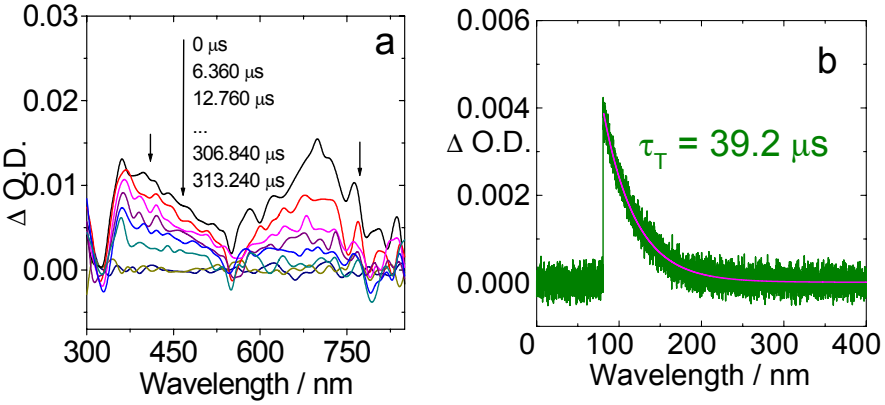

Figure S21. Nanosecond time-resolved transient difference absorption spectra of compounds **RB-C_{60}-2+TFA**. (a) Transient absorption with different delay times (b) decay trace at 450 nm (λ_{ex} = 557 nm), 1.0 × 10^{-5} M, in DCM/MeOH (9/1, v/v) after pulsed laser excitation under N_2 atmosphere, 20 °C.

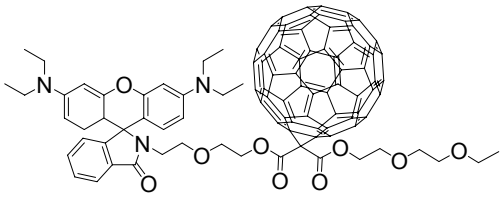

RB-C_{60}-2

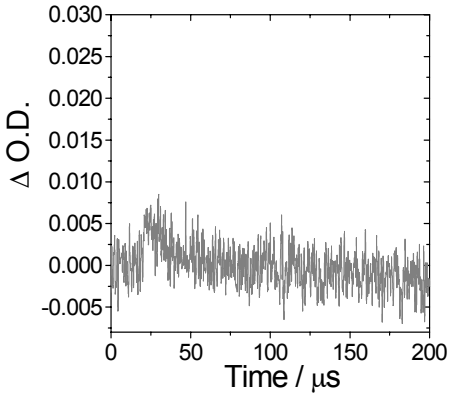

Figure S22. Nanosecond time-resolved transient difference absorption spectra of compounds C_{60}+TFA, decay trace at 720nm (λ_{ex} = 532 nm); c = 1.0 × 10^{-5} M in DCM/MeOH (9/1, v/v) after pulsed laser excitation under N_2 atmosphere, 20 ^{o}C.

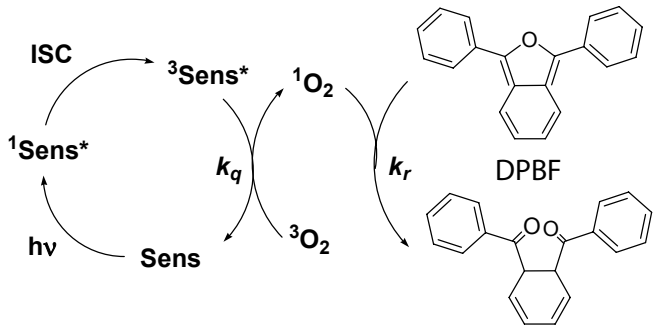

Scheme S2. Mechanism for Monitoring the $^1O_2$ Production of the Dyads with DPBF as $^1O_2$ Scavenger.

8.0 Intracellular ROS Detection upon Irradiation

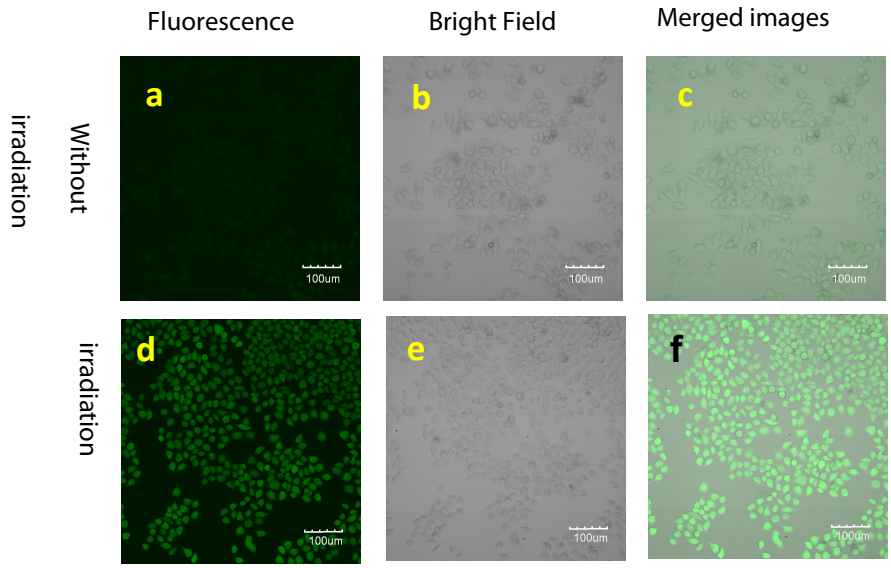

Figure S23. Confocal microscopy images of HeLa cells treated with **RB-C_{60}-1** and DCFH-DA. Cells were incubated with **RB-C_{60}-1** (15.0 μM) for 24 h at 37 °C and then DCFH-DA (10.0 μM) for 2 min before taking the fluorescence image. The excitation wavelength was 488 nm and images were collected at (a, d) 500–530 nm. (b, e) The corresponding contrast image. (c, f) Merged images. No light irradiation was applied for (a-c); Irradiation with 515-525nm light for 3 min was applied for the cells of (d-f). Scale bars: 100 μm.

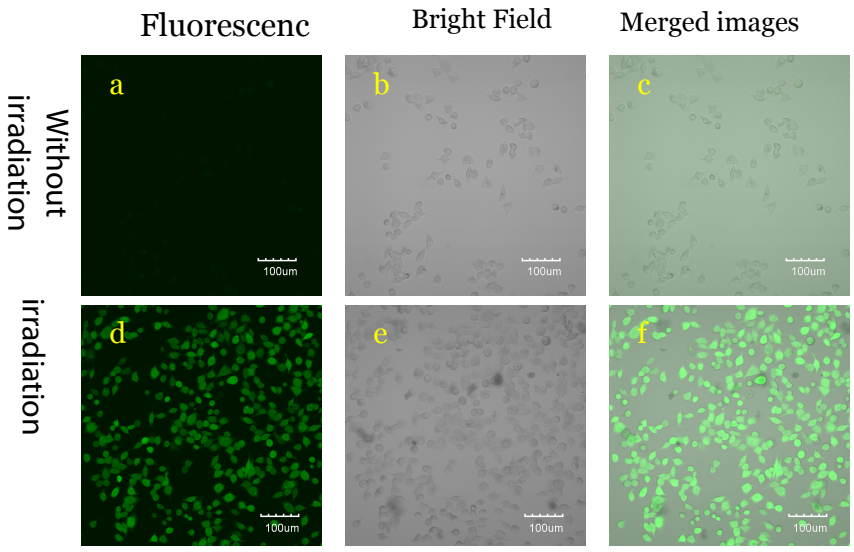

Figure S24. Confocal microscopy images of HeLa cells treated with **RB-C_{60}-2** and DCFH-DA. Cells were incubated with **RB-C_{60}-2** (15.0 μM) for 24 h at 37 °C and then DCFH-DA (10.0 μM) for 2 min before taking the fluorescence image. The excitation wavelength was 488 nm and images were collected at (a, d) 500–530 nm. (b, e) The corresponding contrast image. (c, f) Merged images. No light irradiation was applied for (a-c); Irradiation with 515-525nm light for 3 min was applied for the cells of (d-f). Scale bars: 100 μm.

9.0 Intracellular photodynamic studies

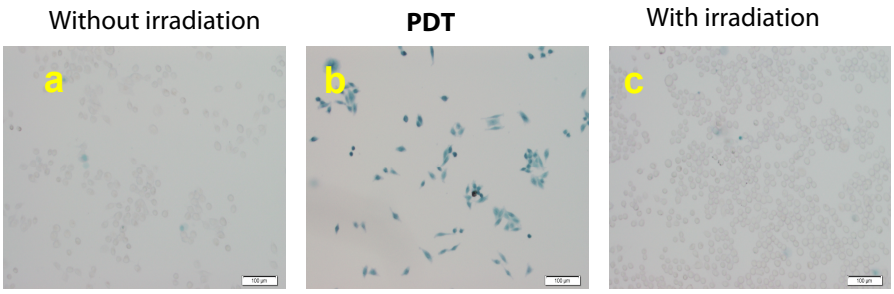

Figure S25. Photocytotoxic activity of the sensitizers with Trypan blue staining images of HeLa cells. (a) Cells were incubated with **RB-C_{60}-1** for 24 h in the darkness; (b) Cells were incubated with **RB-C_{60}-1** for 24 h in the darkness before irradiated with 515-525 nm green LED for 30 min; (c) cells were illuminated for 30 min without the sensitizers and incubated for another 24 h in the darkness. The dead cells are preferentially stained with Trypan blue because of increased cellular permeability. The concentration of **RB-C_{60}-1** was at 15 μM. 37 °C.

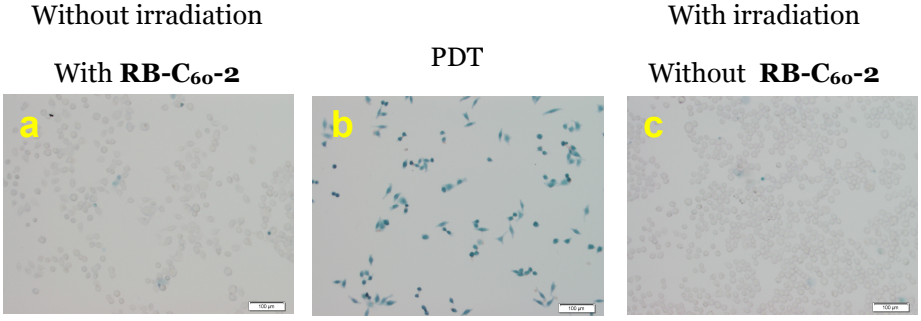

Figure S26. Photocytotoxic activity of the sensitizers with Trypan blue staining images of HeLa cells. (a) Cells were incubated with **RB-C_{60}-2** for 24 h in the darkness; (b) Cells were incubated with **RB-C_{60}-2** for 24 h in the darkness before irradiated with 515-525 nm green LED for 30 min; (c) cells were illuminated for 30 min without the sensitizers and incubated for another 24 h in the darkness. The dead cells are preferentially stained with Trypan blue because of increased cellular permeability. The concentration of **RB-C_{60}-2** was at 15 μM. 37 °C.

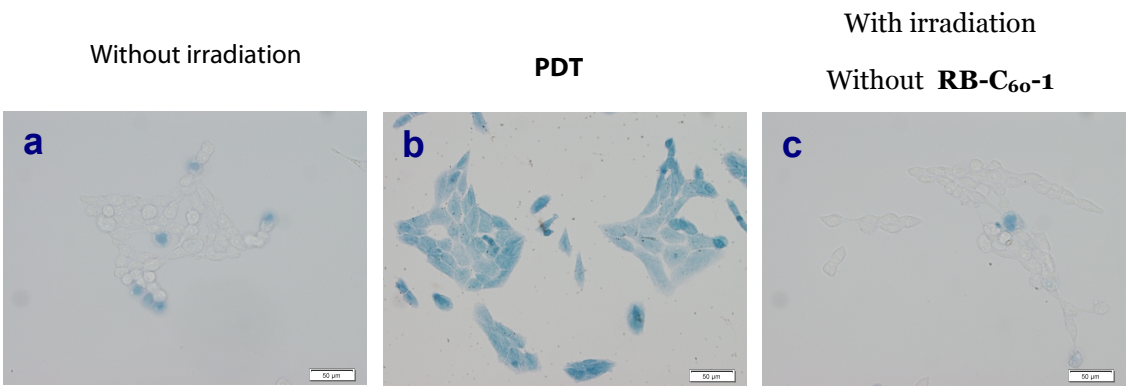

Figure S27. Photocytotoxic activity of the sensitizers on COS-7 cells with Trypan blue staining images. (a) Cells were incubated with **RB-C_{60}-1** for 24 h in the darkness before staining with Trypan blue; (b) Cells were incubated with **RB-C_{60}-1** for 24 h in the darkness before irradiated with 515-525 nm green LED for 30 min and then stained with Trypan blue; (c) cells were illuminated for 30 min without the sensitizers and incubated for another 24 h in the darkness, and stained with Trypan blue. The dead cells are preferentially stained with Trypan blue because of increased cellular permeability. The concentration of **RB-C_{60}-1** was at 15 μM. 37 °C.